Journal of Medicinal Chemistry

ARTICLE

pubs.acs.org/jmc

# A New Phenylalanine Derivative Acts as an Antagonist at the AMPA Receptor GluA2 and Introduces Partial Domain Closure: Synthesis, Resolution, Pharmacology, and Crystal Structure†

Ewa Szymańska,[‡,∥,#] Karla Frydenvang,[‡,#] Alberto Contreras-Sanz,[§] Darryl S. Pickering,[§] Elena Frola,[‡] Zorica Serafimoska,[‡] Birgitte Nielsen,[‡] Jette S. Kastrup,[‡] and Tommy N. Johansen*[,‡]

[‡]Department of Medicinal Chemistry and [§]Department of Pharmacology and Pharmacotherapy, Faculty of Pharmaceutical Sciences, University of Copenhagen, 2 Universitetsparken, DK-2100 Copenhagen, Denmark

Supporting Information

**ABSTRACT:** In order to map out molecular determinants for competitive blockade of AMPA receptor subtypes, a series of 2-carboxyethylphenylalanine derivatives has been synthesized and pharmacologically characterized in vitro. One compound in this series, (*RS*)-**3h**, showed micromolar affinity for GluA1$_o$ and GluA2(*R*)$_o$ receptors with an approximately 4-fold preference for GluA1/2 vs GluA3/4. In TEVC electrophysiological experiments (*RS*)-**3h** competitively antagonized GluA2(*Q*)$_i$ receptors. The X-ray structure of the active enantiomer (*S*)-**3h** in complex with GluA2-S1S2J showed a domain closure around 8°. Even though the nitro and the carboxyethyl groups of (*S*)-**3h** were both anchored to Tyr702 through a water H-bond network, these interactions only induced weak subtype selectivity. In spite of the fact that (*S*)-**3h** induced a domain closure close to that observed for partial agonists, it did not produce agonist responses at GluA2 receptors under nondesensitizing conditions. 2-Carboxyethylphenylalanine derivatives provide a new synthetic scaffold for the introduction of substituents that could lead to AMPA receptor subtype-selective ligands.

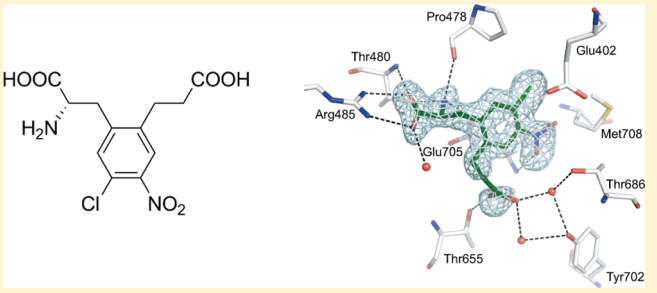


## INTRODUCTION

Ionotropic glutamate receptors (iGluRs) are ligand-gated ion channels that, based on agonist binding affinities and sequence similarities, have been divided into three functionally distinct subclasses: (*RS*)-2-amino-3-(3-hydroxy-5-methylisoxazol-4-yl)-propionic acid (AMPA), kainic acid (KA), and *N*-methyl-D-aspartic acid (NMDA) receptors. Native AMPA receptors, which mediate the majority of the fast excitatory amino acid synaptic transmission in the central nervous system (CNS), are cation-selective tetrameric homo- or heterooligomers formed by combinations of subunits GluA1−4. Across the mammalian brain, a large heterogeneity of AMPA receptors can be observed, differentiated further by splicing of each subunit in an extracellular region (flip and flop variants) that modifies channel kinetics.[1−5] Additional diversity comes from RNA editing of a residue in the pore region of GluA2 from glutamine to arginine, which significantly reduces calcium permeability and decreases single channel conductance in AMPA GluA2-containing receptors[6] and RNA editing of an R/G site controlling channel desensitization properties.[7]

The therapeutic significance of the individual AMPA receptor subunits is not clearly understood, mainly because of lack of potent and selective pharmacological tools. Subunit-selective ligands are therefore valuable, at least as pharmacological tools to investigate the physiological roles of the individual receptor subtypes. Despite a large number of AMPA receptor agonists that have been synthesized and characterized pharmacologically, only few of them have shown high AMPA receptor subunit selectivity.[8] Among the intensively studied class of uracil-based AMPA ligands, (*S*)-5-fluorowillardiine exhibited 55-fold higher potency at GluA1 than GluA3 receptors[9] and a structurally very similar 3-hydroxypyridazine 1-oxide derivative was reported showing 161-fold selectivity for GluA1 over GluA3 receptors.[10] Subunit-selective agonists are also found in the group of isoxazole-based analogues of AMPA. One such ligand is the ibotenic acid derivative (*S*)-2-amino-3-(4-bromo-3-hydroxyisoxazol-5-yl) propionic acid [(*S*)-Br-HIBO, **1**] (Figure 1), a GluA1/2 preferring AMPA receptor agonist with a 70-fold selectivity vs GluA3.[11−13] The corresponding chloro analogue Cl-HIBO exhibited a >1000-fold selectivity.[14] On the basis of detailed structural analyses, it has been claimed[13] that at least part of the marked selectivity among AMPA receptors can be ascribed to interactions between the isoxazole moiety of Br-HIBO and one particular amino acid residue, Tyr698 of GluA1. In GluA2, this residue is conserved (Tyr702), whereas it is a phenylalanine in GluA3 and GluA4.

To the best of our knowledge, similar AMPA receptor subunit selectivity has not yet been identified among competitive antagonists.[8] Even though several structural classes of antagonists are

**Received:** July 1, 2011
**Published:** September 19, 2011

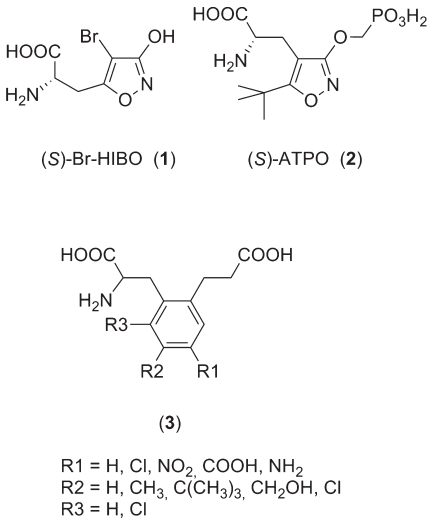


**Figure 1.** Chemical structures of selected AMPA receptor ligands as well as a general structure of the target compounds.

known, a possible reason for the lack of selectivity may be the fact that none of the antagonists occupy the cavity in the neighborhood of Tyr702 in their binding to GluA2. One intensively studied class of competitive antagonists is the isoxazole-based acidic amino acids, of which (*S*)-2-amino-3-[5-*tert*-butyl-3-(phosphonomethoxy)isoxazol-4-yl]propionic acid [(*S*)-ATPO, **2**] is a well-known example. Structural information of the binding of (*S*)-ATPO to the AMPA receptor GluA2 is known (PDB code 1N0T).[15] Analysis of this crystal structure reveals that the isoxazole ring of (*S*)-ATPO, when interacting with the GluA2 ligand binding domain (LBD, GluA2-S1S2), mainly acts as a linker between the $\alpha$-amino acid group and the phosphonate chain. Furthermore, the volume of the binding pocket seems to be large enough to accommodate other spacers, for instance, a phenyl ring, offering possibilities to introduce substituents pointing into different areas of the binding pocket, not accessible when using the isoxazole spacer of (*S*)-ATPO. 2-Substituted phenylalanine-based acidic amino acids have been reported to antagonize AMPA and kainate receptors,[16,17] making such class of compounds a relevant starting point for the design of competitive AMPA receptor antagonists useful for exploring the structural basis for blockade of individual subtypes of AMPA receptors at the molecular level. We therefore synthesized a series of 2-carboxyethylphenylalanine-based acidic amino acids **3** (Figure 1) and solved the X-ray structure of the GluA2 LBD in complex with the most potent compound within the series, **3h**. The pharmacological data were satisfactorily consistent with information derived from the X-ray cocrystal structure which was used to map out some of the molecular determinants defining AMPA receptor subtype selectivity.

## RESULTS

In the target phenylalanines a carboxyethyl chain was introduced into position 2 as a distal acidic group and various substitutions in positions 4, 5, and 6 (in structure **3** R1, R2, and R3, respectively) were examined to explore the available space in the ligand binding cleft. All new target amino acids were pharmacologically characterized by radioligand binding at native AMPA receptors in rat brain membranes and at homomeric recombinant rat AMPA receptors expressed in *Sf*9 insect cell membranes.

**Scheme 1**[a]

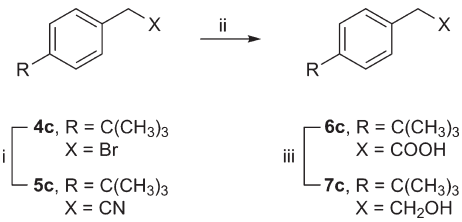


[a] (i) NaCN, DMF, 80 °C; (ii) 60% $H_2SO_4$, reflux; (iii) $LiAlH_4$, THF, 0 °C → reflux.

The most active compound, (*RS*)-2-amino-3-(2-(2-carboxyethyl)-5-chloro-4-nitrophenyl)propionic acid (**3h**), was also examined by two-electrode voltage clamp (TEVC) electrophysiology of AMPA receptors expressed in *X. laevis* oocytes. To investigate the activity of individual enantiomers, **3h** was resolved into *S*- and *R*-enantiomers using chiral HPLC. Finally, (*S*)-**3h** was crystallized in complex with GluA2-S1S2J to 1.9 Å resolution.

**Chemistry.** The syntheses of the new phenylalanine derivatives are illustrated in Schemes 1−5. Starting materials **7b,d** were commercially available, whereas 2-(4-*tert*-butylphenyl)ethanol **7c** was synthesized in three steps from benzyl bromide **4c** (Scheme 1). The target carboxyethyl-substituted phenylalanines **3a**−**d,f,g** were prepared in analogy to a strategy described by Hamilton.[16] Key intermediates, isochromans **8b**−**d**, were prepared from the alcohols **7b**−**d** which were converted into the corresponding MEM-acetals and cyclized to the isochromans using Lewis acids (Scheme 2).

Ring-opening of isochromans **8a**−**d** using 33% HBr in acetic acid, following nucleophilic substitution with diethyl acetamidomalonate under basic conditions, gave bromomalonates **10a**−**d**, which were converted to the corresponding nitriles **11a**−**d** using sodium cyanide. In the case of **11a,c**, dry DMF was used as solvent, resulting in relatively low yields of the substitution products and relatively high yields of corresponding elimination products. For this reason in the cases of **11b,d** the solvent was changed to dry DMSO which markedly increased yields of the expected nitriles and suppressed the elimination reaction. Hydrolysis of **11a**−**d** using aqueous 48% HBr gave the desired amino acids **3a**−**d** as zwitterions either based on treatment with propylene oxide and subsequent crystallization or alternatively using HPLC purification. Compound **12**, obtained as a result of radical bromination of the intermediate nitrile **11b** with NBS, was first refluxed with 48% HBr and then, after evaporation of acid, refluxed for 2 h in water to give amino acid **3e** (Scheme 3).

Preparation of isochromans using the asymmetric alcohol **7f** resulted in an inseparable mixture of the two regioisomers **8f,g** in a 1.6:1 ratio (Scheme 4). The mixture of **8f,g** was then cleaved by 33% HBr in acetic acid to **9f,g** and subsequently treated with diethyl acetamidomalonate to afford a mixture of **10f,g** which could be separated by fractional crystallization from heptane. **10f** and **10g** were finally converted to nitriles **11f,g** and hydrolyzed in analogy to the preparation of **3a**−**d**.

To obtain compounds **3h**−**j**, compound **11d** was treated with a mixture of nitric acid and sulfuric acid in dichloromethane, resulting in nitration exclusively in position 4 of the phenyl ring (Scheme 5). The nitration was accompanied by addition of water to the nitrile. Reduction of the nitro group with iron in the presence of hydrochloric acid gave the corresponding amine **14**, which was converted to **15** in a Sandmeyer reaction using copper

cyanide. Hydrolysis of intermediates **13**, **14**, and **15** and purification in analogy to the preparation of **3a**−**d** afforded the target amino acids **3h**−**j**.

**Chromatographic Resolution of 3h.** Resolution of racemic **3h** was performed by chiral HPLC using a Sumichiral OA-5000 ligand-exchange column containing *N*,*S*-dioctyl-D-penicillamine[18,19] as chiral selector to give the *R*- and *S*-enantiomers of **3h** with the satisfactory enantiomeric excess (ee): (*R*)-**3h**, 95% ee; (*S*)-**3h**, 97% ee. The ee of the isolated enantiomers was determined using a Chirobiotic T column.[20,21] The first eluting enantiomer on the Sumichiral column was also the first eluting enantiomer on the Chirobiotic column. This elution order, supported by the previously reported elution orders of a number of $\alpha$-amino acids (including the structurally related amino acids Phe and Tyr) on both the Sumichiral column[19,22] and the Chirobiotic T column,[20,21,23] strongly suggests that the first eluting enantiomer on the Sumichiral column has *S*-configuration. To strengthen this configurational assignment, CD spectra were recorded for both enantiomers and for (*S*)-Phe as a reference compound. Similar to (*S*)-Phe, the less retained enantiomer showed a positive Cotton effect at 205 nm ($\Delta\varepsilon$ = 0.44 m$^2$/mol), which is in agreement with published data observed for (*S*)-$\alpha$-amino acids in acidic solution.[24]

**Binding Pharmacology.** Compounds **3a**−**j** were evaluated at native and cloned AMPA receptors in radioligand binding assays (Tables 1 and 2). Among this series, compound **3h** (R1 = $NO_2$; R2 = Cl; R3 = H; Table 1) was found to have low micromolar affinity at native AMPA receptors, compounds **3b**,**d**−**f** showed high micromolar affinities, while compounds **3a**,**c**,**g** did not show detectable affinity. Compound **3h** was subsequently characterized at all the cloned rat GluA1−4 (flop isoforms), as well as at the soluble GluA2 constructs[25] GluA2-S1S2J and (Y702F)GluA2-S1S2J (Table 2). Hill coefficients were near unity at all receptors, indicating binding to a single population of sites in each case. A 4-fold difference in affinity at GluA1/2 vs GluA3/4 was observed for **3h** ($P < 0.05$, one way ANOVA, Bonferroni post-test); however, the affinity was not statistically significantly different between full-length GluA2($R$)$_o$, construct GluA2-S1S2J, or (Y702F)GluA2-S1S2J ($P = 0.233$, one way ANOVA). This suggests that, in contrast to the situation with Br-HIBO, this Y/F amino acid position is not critical for the observed binding affinity profile of **3h**. However, the full-length receptor mutant (Y716F)GluA1$_o$ did exhibit an increased $K_i$ for **3h**, suggesting that the Y/F position can contribute to the GluA1/2 vs GluA3/4 preference of **3h**.

**Functional Pharmacology.** By use of TEVC electrophysiology, the antagonist properties of the enantiomers of **3h** were examined at homomeric GluA2($Q$)$_i$ and GluA3$_i$ expressed in *X. laevis* oocytes (Table 3). (*RS*)-**3h** dose-dependently antagonized the responses to (*S*)-Glu (Figure 2) and exhibited only a 2.4-fold selectivity in the calculated $K_b$ values toward GluA2($Q$)$_i$ vs GluA3$_i$ ($P < 0.001$, Student's $t$ test). Slopes of (*RS*)-**3h** concentration−response inhibition curves were close to unity. The functional $K_b$ values of (*RS*)-**3h** at GluA2($Q$)$_i$ and GluA3$_i$ (Table 3) were not statistically significantly different from their respective $K_i$ values determined from radioligand binding experiments ($P > 0.05$, one way ANOVA, Bonferroni post-test) (Table 2). The activity of **3h** resides in the *S*-enantiomer, which had a calculated $K_b$ at GluA2($Q$)$_i$ of approximately one-half that of the racemate, while the low potency observed for (*R*)-**3h** (95% ee) was in good agreement with the observed percentage of the *S*-enantiomer left after recrystallization, supporting (*R*)-**3h** as being inactive as an antagonist. A rightward shift in the (*S*)-Glu concentration−response curve with unchanged maximal response indicates competitive antagonism by **3h** (Figure 3).

**Scheme 2**[a]

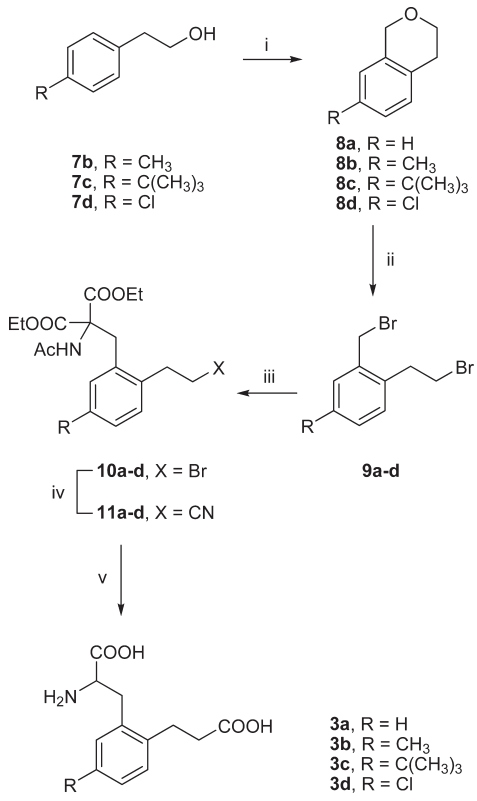


[a] (i) (1) MEM-chloride, DIPEA, $CH_2Cl_2$, room temp; (2) $TiCl_4$, $CH_2Cl_2$, 0 °C; (ii) 33% HBr in AcOH, 110 °C; (iii) NaH, 1.1 equiv, diethyl acetamidomalonate, 1.1 equiv, DMF, room temp; (iv) NaCN, DMF or DMSO, 80 °C; (v) 48% HBr, reflux.

**Scheme 3**[a]

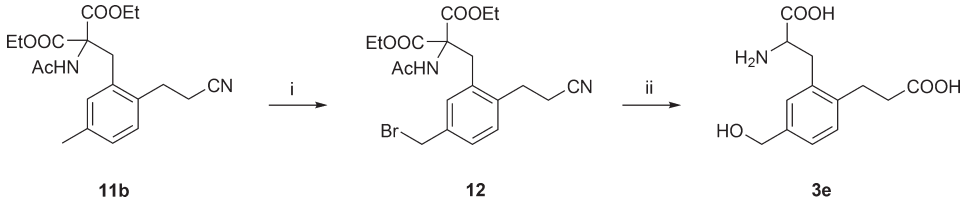


[a] (i) NBS, benzoyl peroxide, $CCl_4$, reflux; (ii) (1) 48% HBr, reflux, (2) $H_2O$, reflux.


dx.doi.org/10.1021/jm200862h |*J. Med. Chem.* 2011, 54, 7289–7298

**Scheme 4**[a]

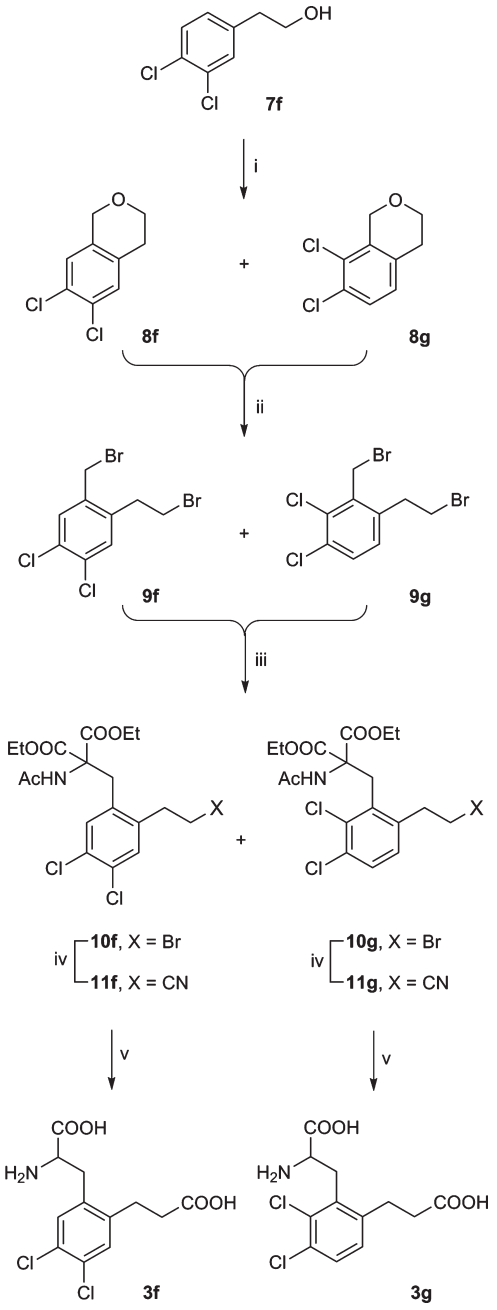


[a] (i) (1) MEM-chloride, DIPEA, $CH_2Cl_2$, rt; (2) $TiCl_4$, $CH_2Cl_2$, 0 °C; (ii) 33% HBr in AcOH, 110 °C; (iii) NaH, 1.1 equiv, diethyl acetamidomalonate, 1.1 equiv, DMF, room temp; (iv) NaCN, DMF, 80 °C; (v) 48% HBr, reflux.

Application of 600 $\mu$M (*S*)-**3h** plus 100 $\mu$M cyclothiazide did not produce any detectable agonist response at GluA2(*Q*)$_i$ (Figure 4). In some experiments, at very negative holding potentials, extremely tiny responses to **3h** were observed yielding an estimated efficacy of <0.005 compared to that for (*S*)-Glu.

**X-ray Crystallographic Analysis.** The X-ray structure of the compound (*S*)-**3h** bound to GluA2-S1S2J was solved to 1.9 Å resolution. The GluA2-S1S2J construct comprises a Gly-Ala cloning remnant, amino acid residues 392−506 from segment S1 of the membrane-bound receptor, a two amino acid linker Gly-Thr, and residues 632−775 from segment S2 (numbering without signal peptide). The complex was crystallized as a dimer with the ligand (*S*)-**3h** observed in both binding clefts. In both molA and molB all residues could be modeled, as well as Ala from the cloning remnant in the N-terminal end of molA. Experimental procedures including a summary of data collection and structure refinements are presented in Supporting Information.

The binding mode of (*S*)-**3h** to the GluA2 receptor construct (Figure 5a) to some extent resembles that of other amino acid based competitive antagonists.[15,26] The $\alpha$-carboxyl and $\alpha$-amino groups of (*S*)-**3h** are observed at exactly the same position in the GluA2 binding cleft and show the same type of hydrogen bonding interactions as in case of (*S*)-ATPO[15] and as reported more recently for two willardiine-based antagonists.[26] However, the position of the carboxyethyl chain of (*S*)-**3h** differs from that observed for phosphonate in the GluA2-S1S2J:(*S*)-ATPO complex with a bent conformation of the carboxyethyl side chain that places the distal carboxylate group in a relatively wide hydrophilic pocket in the vicinity of Thr655, Thr686, and Tyr702 (Figure 5b). Apart from the direct hydrogen bond with Thr655, the distal carboxylate group is involved in interactions with surrounding residues, mediated by a water-mediated H-bonding network (Figure 5a). The electron density of the carboxyethyl moiety is weak and thus indicates flexibility of the substituent, even when bound to the receptor (Figure 5a). This flexibility results in a slightly different conformation of the ligand in molA and molB.

The nitro substituent of (*S*)-**3h** is accommodated by a cavity formed by Thr686, Leu704, Glu705, and Met708 (Figure 5b), directly interacting, by one of its oxygen atoms, with the backbone NH of Glu705 (Figure 5a). The same oxygen atom makes a weak hydrogen bond (3.4 Å) to Thr686 and Tyr702 through a water molecule that is engaged in H-bond formation between the carboxylate of (*S*)-**3h** and the side chain hydroxyl group of Tyr702 (Figure 5a). Apparently, the second oxygen atom of the nitro group is not involved in any hydrogen bond, which might explain why no electron density is observed for this atom.

The chlorine atom of (*S*)-**3h**, located in a pocket between residues of the domains D1 and D2 (Figure 5b), together with the nitro group forces the Met708 side chain away from the binding cleft because of otherwise steric repulsions. In addition, the presence of both chlorine and nitro substituents prohibits interdomain "locking"[15] by preventing formation of the important hydrogen bond between Glu402 in D1 and Thr686 in D2 (distance is 4.5 Å, Figure 5a), which consequently prevents domain closure.

## DISCUSSION

A new series of phenylalanine-based AMPA receptor antagonists has been designed from the structure of the isoxazole-based acidic amino acid (*S*)-ATPO and the X-ray structure of (*S*)-ATPO cocrystallized with GluA2-S1S2J. Replacing the five-membered isoxazole heterocycle with a larger phenyl spacer between the alanyl part and the distal acidic functionality has allowed for a study of the effect of introducing substituents pointing into different areas of the binding pocket. This new series of compounds shows a structure−activity relationship with some similarities to, but also some differences from, that observed for the well-studied isoxazole-based antagonists.[27]

In order to analyze in detail structural factors influencing the pharmacological profile of the presented series of 2-carboxyethylphenylalanines, the crystal structure was solved for GluA2-S1S2J


dx.doi.org/10.1021/jm200862h |*J. Med. Chem.* 2011, 54, 7289–7298

**Scheme 5**[a]

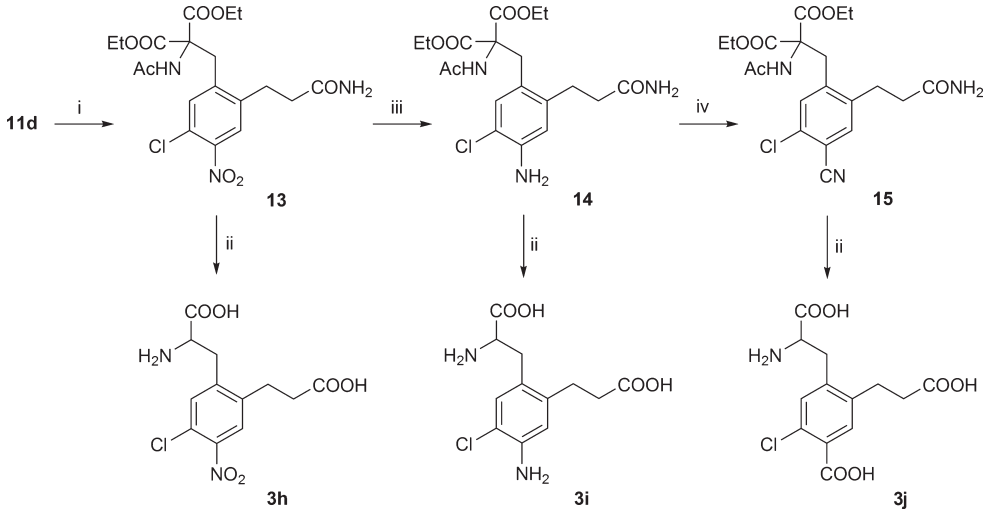


[a] (i) 100% $HNO_3$, 96% $H_2SO_4$, $CH_2Cl_2$, 0 °C; (ii) 48% HBr, reflux; (iii) Fe, 35% HCl, ethanol, water, 90 °C; (iv) (1) 30% HCl, $NaNO_2$, −10 °C, (2) $CuSO_4$, KCN, aqueous $NH_3$, 0 °C.

**Table 1. Binding Pharmacology at Native Rat Brain Membranes Using [$^3$H]AMPA as Radioligand**[a]

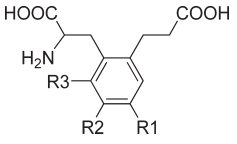


| compd | R1 | R2 | R3 | $IC_{50}$ ($\mu$M) |
|---|---|---|---|---|
| **3a** | H | H | H | >100 |
| **3b** | H | $CH_3$ | H | 74 ± 7 |
| **3c** | H | $C(CH_3)_3$ | H | >100 |
| **3d** | H | Cl | H | 61 ± 4 |
| **3e** | H | $CH_2OH$ | H | 63 ± 4 |
| **3f** | Cl | Cl | H | 19 ± 1 |
| **3g** | H | Cl | Cl | >100 |
| **3h** | $NO_2$ | Cl | H | 3.4 ± 0.3 |
| **3i** | $NH_2$ | Cl | H | >100 |
| **3j** | COOH | Cl | H | >100 |

[a] Mean ± SEM values are indicated for selected compounds from at least three separate experiments, conducted in triplicate.

**Table 2. Binding Pharmacology of 3h at Cloned rat GluA1−4 Expressed in *Sf9* Insect Cell Membranes or As Soluble Ligand Binding Domain Constructs (S1S2J)**[a]

| receptor | $K_i$ ($\mu$M) | $n_H$ |
|---|---|---|
| $GluA1_o$ | 6.87 ± 0.62 | 0.92 ± 0.04 |
| $(Y716F)GluA1_o$ | 15.5 ± 1.1 | 1.13 ± 0.23 |
| $GluA2(R)_o$ | 4.36 ± 0.53 | 0.92 ± 0.07 |
| GluA2-S1S2J | 3.15 ± 0.64 | 1.02 ± 0.07 |
| (Y702F)GluA2-S1S2J | 3.06 ± 0.39 | 1.15 ± 0.03 |
| $GluA3_o$ | 22.7 ± 3.2 | 0.92 ± 0.10 |
| $GluA4_o$ | 20.4 ± 3.4 | 0.85 ± 0.03 |

[a] Mean ± SEM are shown from at least three separate experiments, conducted in triplicate at 16 ligand concentrations. $n_H$ is the Hill coefficient.

bound to the most active compound, (*S*)-**3h**. During the past decade several X-ray complexes of GluA2-S1S2J have been reported[28] in which the receptor construct has been cocrystallized together with a number of structurally different amino acid based[15,26] or quinoxalinedione-related[29−32] competitive antagonists, such as 6-cyano-7-nitroquinoxaline-2,3-dione (CNQX). Comparison of the binding interactions of (*S*)-ATPO and CNQX with the GluA2 binding pocket suggests that (*S*)-**3h** resembles a hybrid of (*S*)-ATPO and CNQX (Figure 6). The $\alpha$-carboxylate and $\alpha$-ammonium groups of (*S*)-**3h** interact through hydrogen bonds and ion-pair interactions with the protein in the same way as described for (*S*)-ATPO, reproduced in the case of CNQX by two carbonyl groups and one of the quinoxaline nitrogen atoms. However, the position of the carboxyethyl chain of (*S*)-**3h** differs from that observed for the phosphonate moiety in the GluA2-S1S2J:(*S*)-ATPO complex. Instead of direct contacts with residues of D2, the distal carboxylate of (*S*)-**3h** interacts directly only with Thr655 and is also involved in an extensive network of hydrogen bonds formed with the receptor protein through water molecules.

The chlorine atom in the R2 position of (*S*)-**3h** corresponds to the cyano group of CNQX and *tert*-butyl group of (*S*)-ATPO (Figure 6); all these groups fill the same, partly polar partly hydrophobic cavity formed by residues of D1 and D2. The nitro substituent of (*S*)-**3h** nearly occupies the same position in the binding cleft as the nitro group in CNQX. In contrast to CNQX, however, one of the oxygen atoms of the nitro substituent of (*S*)-**3h** does not interact directly with Thr686 but makes a weak hydrogen bond with a water molecule which mediates contacts with Thr686 and Tyr702.

Analysis of available X-ray structures of GluA2-S1S2J with various ligands shows that, relative to the apo structure,[29] full agonists such as (*S*)-Glu and (*S*)-AMPA induce full domain closure (approximately 21°),[29] while partial agonists such as kainic acid and


dx.doi.org/10.1021/jm200862h |*J. Med. Chem.* 2011, 54, 7289–7298

**Table 3. TEVC Pharmacology of 3h at Cloned Rat AMPA Receptors Expressed in *X. laevis* Oocytes**[a]

| | $K_b$ ($\mu$M) | | |
|---|---|---|---|
| receptor | (*RS*)-**3h** | (*S*)-**3h** | (*R*)-**3h** |
| GluA2($Q$)$_i$ | 8.59 ± 0.70 (12) | 3.43 ± 0.42 (9) | 57.7 ± 19.0 (3) |
| GluA3$_i$ | 20.4 ± 1.4 (9) | nd | nd |

[a] Shown are mean ± SEM values of duplicate measurements at 8−10 concentrations; number of experiments is in parentheses. nd, not determined.

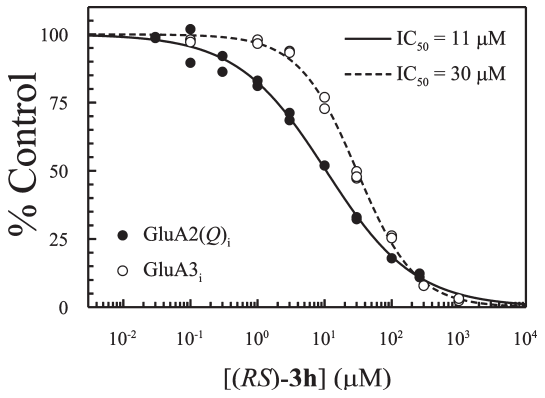


**Figure 2.** Antagonism of (*S*)-Glu (3 $\mu$M) responses at GluA2($Q$)$_i$ and GluA3$_i$ by (*RS*)-**3h**. Shown are results from representative TEVC experiments, conducted with duplicate stimulations. The control response is 3 $\mu$M (*S*)-Glu in the absence of antagonist. $V_h$ = −45 mV (GluA2($Q$)$_i$); $V_h$ = −90 mV (GluA3$_i$).

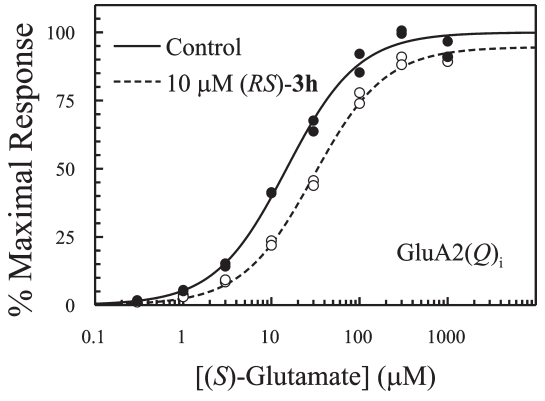


**Figure 3.** Concentration−response curves of (*S*)-Glu in the absence (control) and presence of 10 $\mu$M (*RS*)-**3h** in an oocyte expressing GluA2($Q$)$_i$, which indicate competitive antagonism. Currents are expressed as a percentage of the maximal control response. Stimulations were carried out in duplicate at $V_h$ = −60 mV: ○, $EC_{50}$ = 15 $\mu$M; ●, $EC_{50}$ = 30 $\mu$M.

Br-HIBO induce domain closure in the range of 12−18°.[13,29] On the other hand, competitive antagonists, as CNQX and (*S*)-ATPO, hold the LBD of GluA2 in an open conformation, showing small domain closures (from 3−8°)[15,29−31] or even small domain opening as 8-methyl-5-(4-(*N*,*N*-dimethylsulfamoyl)phenyl)-6,7,8,9,-tetrahydro-1*H*-pyrrolo[3,2-*h*]isoquinoline-2,3-dione-3-*O*-(4-hydroxybutyrate-2-yl)oxime (NS1209) (5°).[32] The domain closure induced by (*S*)-**3h** is 9° in molA and 7° in molB. This means that compared to (*S*)-ATPO (3−5°)[15] and CNQX

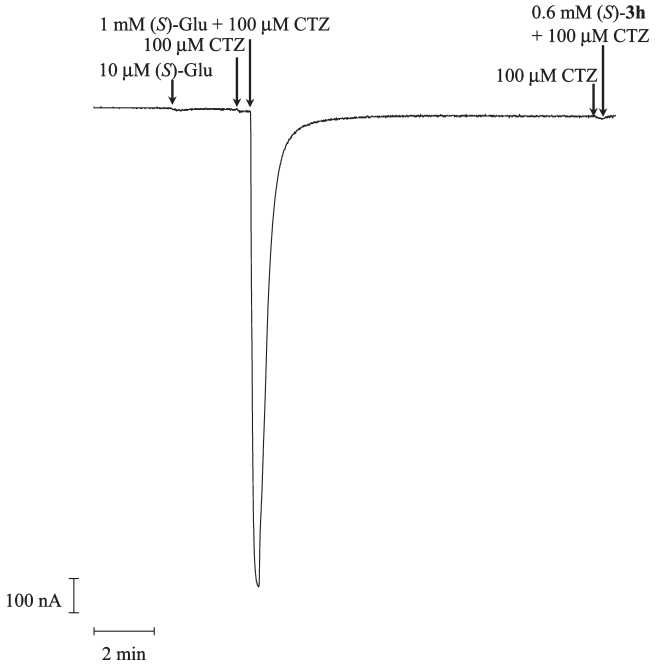


**Figure 4.** Lack of agonist response by (*S*)-**3h** at GluA2($Q$)$_i$ under nondesensitizing conditions (100 $\mu$M cyclothiazide, CTZ). $V_h$ = −30 mV. Drug application duration is 30−45 s.

(6−8°),[30] (*S*)-**3h** holds the binding cleft of GluA2 in a slightly tighter conformation, showing a domain closure in close range to those induced by partial agonists. In light of this observation it should be emphasized that no clear sign of agonism was observed for (*S*)-**3h** in electrophysiological studies performed under conditions where desensitization was blocked with 100 $\mu$M cyclothiazide (Figure 4), although a very low efficacy partial agonism cannot be completely ruled out. In this context, it is interesting to note that CNQX has been shown to be a partial agonist in the presence of transmembrane AMPA receptor regulatory proteins.[30]

Further comparison of the binding modes of (*S*)-ATPO, CNQX, and (*S*)-**3h** shows that the nitro group in the R1 position and the chlorine atom in the R2 position interfere with the D1−D2 interdomain hydrogen bond between Glu402 and Thr686, preventing the formation of this D1−D2 lock in a way similar to CNQX. It has been shown that the D1−D2 interdomain lock contact plays an important role in the agonist-induced closed conformation.[13,33] In the crystal structure of (*S*)-**3h** the stabilization of an open LBD conformation is reinforced by direct, as well as water-mediated, interactions of the distal carboxylate group of (*S*)-**3h** with residues of D2 (Thr655, Thr686, and Tyr702), similar to interactions seen in case of (*S*)-ATPO.[15]

Using the X-ray structure of (*S*)-**3h** in complex with GluA2-S1S2J for a structure−affinity analysis reveals possible explanations for the observed binding affinities. In the first series of compounds with both R1 and R3 positions of the phenyl ring unsubstituted (**3a**−**e**, Table 1), it appears that substituents of intermediate size such as methyl (**3b**), chloro (**3d**), and hydroxymethyl (**3e**) are equally well accommodated by the receptor. The chloro substituent in position R2 of **3h** is nearly overlying the *tert*-butyl group of (*S*)-ATPO (Figure 6), but whereas the *tert*-butyl of (*S*)-ATPO appears to be optimal for AMPA receptor affinity,[15,27] the same bulky substituent of **3c** appears to be too large (Table 1).

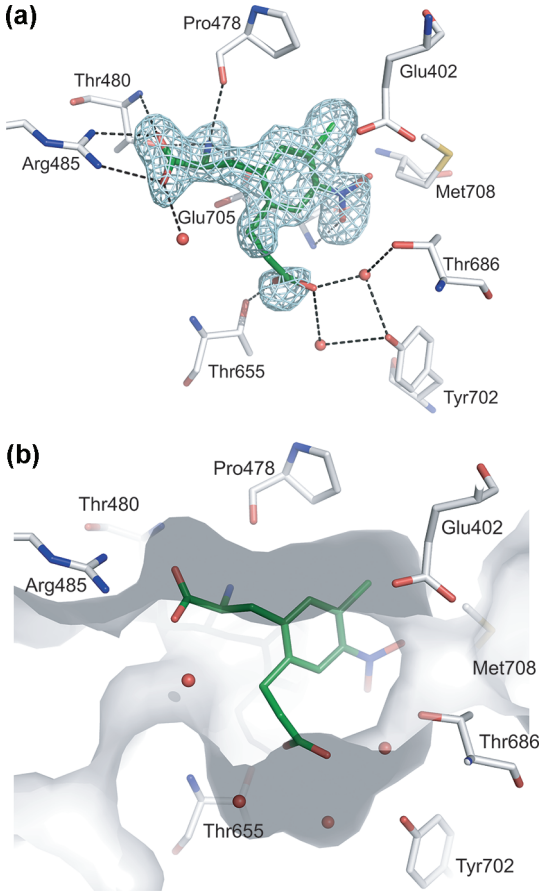


**Figure 5.** Binding mode of (*S*)-**3h** in the ligand binding site of GluA2-S1S2J. (A) Omit $F_o - F_c$ electron-density map contoured at the 3$\sigma$ level. Polar contacts (dashed lines) to the ligand (*S*)-**3h** within 3.2 Å are shown as well as the water-mediated network between the ligand and Tyr702. Residues of GluA2-S1S2J (molA) are represented as white sticks and water molecules as red spheres. (B) Surface of the ligand binding cavity (shown in white), illustrating the flexibility of the cavity and the extra volume occupied by water molecules. Water molecules within 3.5 Å from the ligand are shown.

Among the group of phenylalanine derivatives with R2 = Cl, R3 = H and a variety of substituents in the R1 position (**3d**, **3f**, **3h**–**j**, Table 1) it was observed that introducing an additional Cl substituent (**3f**, R1 = Cl) or a nitro group (**3h**, R1 = $NO_2$) was beneficial for the affinity (Table 1), the nitro group being superior. Whereas the nitro group of **3h** is a H-bond acceptor and contributes to favorable interactions with GluA2 residues and water molecules (Figure 5a), the R1 chlorine atom of **3f** is also capable of accepting hydrogen bonds; however, the hydrogen bonds are expected to be longer and therefore weaker than for the nitro group. The fact that compounds **3f** and **3h** accept hydrogen bonds with a dissimilar spatial orientation might contribute to the difference in affinity observed for the two compounds. Compound **3d** has a hydrogen atom instead of a nitro group and is therefore unable to take part in a hydrogen bonding network similar to **3h**, which most likely explains the weaker binding of **3d** compared to **3f** and **3h**. Compounds with an amino or a carboxy group in position R1 (**3i** and **3j**, respectively) only showed limited binding to native AMPA receptors ($IC_{50}$ > 100 $\mu$M). The aromatic amine in **3i** can act as a hydrogen bond donor for the water molecule but cannot function as a hydrogen bond acceptor (from the backbone NH of Glu705). In the case of **3j**, a likely explanation for the lack of affinity is related to the fact that a carboxylate group in the R1-position is unfavorable in this part of the receptor cavity because of a nearby carboxylate (Glu402); thus, binding of **3j** will result in charge–charge repulsion. Finally, substitution with an additional chlorine atom in the R3 position (**3g**) is not tolerated by the receptor, probably because of too close contacts in the region of Pro478 and Tyr450.

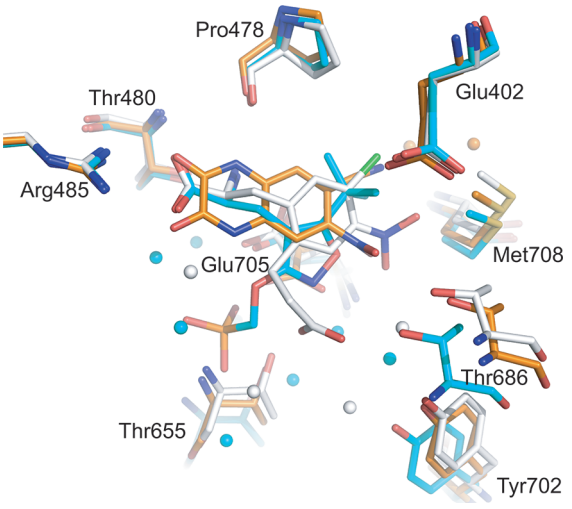


**Figure 6.** Superimposition of the binding mode of three competitive antagonists. The structures of GluA2-S1S2J with (*S*)-**3h** (white), (*S*)-ATPO (cyan), and CNQX (orange) have been superimposed on D1 residues (all molA). Water molecules (within 3.5 Å) are displayed in colors according to the ligands.

Despite a large number of AMPA receptor ligands that have been synthesized and characterized pharmacologically, only few of them have shown high AMPA receptor subunit selectivity.[11,12,14] For agonists it has previously been claimed that such a selectivity profile within AMPA receptors at least partly can be ascribed to water-mediated interactions between the ligands and Tyr702 in GluA2 (Tyr698 in GluA1).[13] This interaction is unavailable in GluA3 and GluA4, where the corresponding residue is Phe. For this reason we decided to carry out detailed binding studies of (*S*)-**3h** both to homomeric GluA1–4 receptors and to the soluble constructs GluA2-S1S2J and (Y702F)GluA2-S1S2J mutant. (*S*)-**3h** displayed a weak GluA1/GluA2 over GluA3/GluA4 selectivity. However, no difference in binding affinity to both constructs was observed showing that this single residue alone cannot account for the difference in binding affinity of **3h** between GluA1/GluA2 and GluA3/GluA4 full-length receptors. In conclusion, we have identified a competitive AMPA receptor antagonist, (*S*)-**3h**, that induces a domain closure of GluA2 greater than that observed for CNQX. Even though the domain closure induced by (*S*)-**3h** is close to that observed for partial agonists, such as KA, (*S*)-**3h** does not show any agonist response at GluA2 receptors. However, (*S*)-**3h** and its interactions with GluA2-S1S2J might be useful elements for future studies mapping out important molecular interactions and conformational changes of the receptor protein for receptor activation and blockade.

## EXPERIMENTAL SECTION

**Chemistry. General Procedures.** All solvents and reagents were purchased from commercial sources and used without further purification. Analytical thin-layer chromatography (TLC) was performed


dx.doi.org/10.1021/jm200862h |*J. Med. Chem.* 2011, 54, 7289–7298

on silica gel 60 $F_{254}$ aluminum plates (Merck). All compounds were detected using UV light and a $KMnO_4$ spraying reagent. The target amino acids were also visualized using a ninhydrin spraying reagent. $^1$H NMR spectra were recorded on a 300 MHz Varian Mercury 300BB or 300 MHz Varian Gemini 2000BB spectrometer. $D_2O$ or DMSO-$d_6$ (dimethyl-$d_6$-sulfoxide) were used as solvents. Chemical shifts ($\delta$) are given in parts per million (ppm), and coupling constants ($J$) are given in hertz (Hz). The following abbreviations were used: br s = broad singlet, s = singlet, d = doublet, dd = double doublet, t = triplet, m = multiplet. Elemental analyses were performed by J. Theiner, Microanalytical Laboratory, Department of Physical Chemistry, University of Vienna, Austria, and are within ±0.5% of the theoretical values, corresponding to ≥95% purity. CD spectra of (*R*)- and (*S*)-**3h** were recorded at ambient temperature in 1.0 cm cuvettes on an OLIS DSM (digital subtractive method) 10 CD spectrophotometer dissolved in 1 M HCl/ethanol (1:1).

**HPLC Procedures.** Preparative chromatography was performed using HPLC system consisting of a Jasco 880-PU pump, a Rheodyne 7125 injector equipped with a 5.0 mL sample loop, a Shimadzu SPD-6A detector (220 or 250 nm), and a Merck-Hitachi D-2000 chromato-integrator. Purification of target amino acids was performed on a reversed-phase Xterra MS $C_{18}$ column, 10 $\mu$m, 10 mm × 300 mm, Waters. The column was isocratically eluted at 8 mL/min with a mixture of methanol and 15 mM aqueous AcOH, the concentration of methanol varying depending on the structure of the target amino acid. Preparative resolution of the racemic **3h** was performed using the Sumichiral OA-5000 chiral ligand exchange column (10 mm × 250 mm) equipped with a Sumichiral OA-5000 guard column (10 mm × 4 mm, Sumika Chemical Analysis Service, Japan). The column was eluted at 4 mL/min with a mixture of 2-propanol (15% v/v) and an aqueous solution of ammonium acetate (50 mM), adjusted to pH 4.7 with glacial AcOH and containing copper(II) acetate (0.1 mM). The temperature of column was kept at 60 °C. Determination of the enantiomeric excess (ee) of (*R*)- and (*S*)-**3h** was performed on a Chirobiotic T column (4.6 mm × 150 mm, ASTEC) equipped with a Chirobiotic T guard column (4.6 mm × 50 mm, ASTEC). Elution was performed with 0.5 mL/min of a mixture of water adjusted to pH 4 with AcOH and ethanol (40:60).

**Final Steps in the Synthesis of Compounds 3a−c,f,g.** A mixture of **11** (0.5 mmol) and 48% HBr in water (3 mL) was refluxed for 2 h, then evaporated under reduced pressure. The residue was dissolved in water (10 mL), washed with diethyl ether (10 mL), and the water phase was evaporated in vacuo. The remaining solid was dissolved in a mixture of ethanol and water (7:3), and the pH was raised to the isoelectric point (pH 4−5) by adding propylene oxide. The precipitated crystals were filtered, dried, and recrystallized from ethanol−water (3:1) (**3a**) or from water (**3b,c,f,g**) to give white crystals of the target amino acid.

**(*RS*)-2-Amino-3-(2-(2-carboxyethyl)phenyl)propionic Acid (3a).** Yield 51 mg, 43%. Anal. Calcd for $C_{12}H_{15}NO_4 \cdot 0.65H_2O$: C, 57.89; H, 6.60; N, 5.63. Found: C, 57.86; H, 6.46; N, 5.51. $^1$H NMR (300 MHz, $D_2O$): $\delta$ 2.41 (t, $J$ = 7.2 Hz, 2H, $CH_2$), 2.68 (t, $J$ = 7.2 Hz, 2H, $CH_2$), 2.92 (dd, $J_1$ = 14.7 Hz, $J_2$ = 8.9 Hz, 1H, CHH), 3.17 (dd, $J_1$ = 14.7 Hz, $J_2$ = 6.5 Hz, 1H, CHH), 4.04 (dd, $J_1$ = 8.9 Hz, $J_2$ = 6.5 Hz, 1H, CH), 7.00−7.11 (m, 4H, Ar). $^{13}$C NMR (75 MHz, $D_2O$): $\delta$ 26.5, 32.9, 34.4, 53.8, 127.1, 128.2, 129.9, 130.4, 132.1, 139.2, 171.3, 177.9.

**(*RS*)-2-Amino-3-(2-(2-carboxyethyl)-5-methylphenyl)propionic Acid (3b).** Yield 84 mg, 67%. Anal. Calcd for $C_{13}H_{17}NO_4 \cdot 0.8H_2O$: C, 58.77; H, 7.06; N, 5.27. Found: C, 58.47; H, 6.97; N, 5.57. $^1$H NMR (300 MHz, $D_2O$): $\delta$ 2.04 (s, 3H, $CH_3$), 2.42 (t, $J$ = 7.4 Hz, 2H, $CH_2$), 2.70 (t, $J$ = 7.4 Hz, 2H, $CH_2$), 2.78 (dd, $J_1$ = 14.0 Hz, $J_2$ = 8.9 Hz, 1H, CHH), 3.10 (dd, $J_1$ = 14.0 Hz, $J_2$ = 6.2 Hz, 1H, CHH), 3.69 (dd, $J_1$ = 8.9 Hz, $J_2$ = 6.2 Hz, 1H, CH), 6.85 (s, 1H, Ar), 6.89 (d, $J$ = 8.3 Hz, 1H, Ar), 6.95 (d, $J$ = 7.8 Hz, 1H, Ar). $^{13}$C NMR (75 MHz, $D_2O$): $\delta$ 20.2, 26.3, 32.9, 34.8, 53.7, 129.0, 129.3, 131.0, 132.0, 136.0, 137.1, 171.2, 177.4.

**(*RS*)-2-Amino-3-(5-*tert*-butyl-2-(2-carboxyethyl)phenyl)propionic Acid (3c).** Yield 69 mg, 47%. Anal. Calcd for $C_{16}H_{23}NO_4$: C, 65.51; H, 7.90; N, 4.77. Found: C, 65.18; H, 7.84; N, 4.71. $^1$H NMR (300 MHz, DMSO-$d_6$): $\delta$ 1.27 (s, 9H, $CH_3$), 2.45−2.55 (m, 2H, $CH_2$), 2.75−2.94 (m, 3H, $CH_2$ and CHH), 3.25 (dd, $J_1$ = 14.7 Hz, $J_2$ = 4.5 Hz, 1H, CHH), 3.43 (dd, $J_1$ = 7.8 Hz, $J_2$ = 4.5 Hz, 1H, CH), 7.12 (d, $J$ = 8.1 Hz, 1H, Ar), 7.20 (dd, $J_1$ = 8.1 Hz, $J_2$ = 2.1 Hz, 1H, Ar), 7.29 (d, $J$ = 1.8 Hz, 1H, Ar). $^{13}$C NMR (75 MHz, $D_2O$, as a hydrobromide salt): $\delta$ 28.7, 33.2, 35.9, 36.5, 37.2, 56.3, 127.8, 130.3, 131.5, 134.2, 138.6, 152.7, 173.7, 179.7.

**(*RS*)-2-Amino-3-(2-(2-carboxyethyl)-4,5-dichlorophenyl)propionic Acid (3f).** Yield 96 mg, 63%. Anal. Calcd for $C_{12}H_{13}NO_4Cl_2$: C, 47.08, H, 4.28, N, 4.58; Found: C, 46.99; H, 4.46; N, 4.46. $^1$H NMR (300 MHz, DMSO-$d_6$): $\delta$ 2.50 (td, $J_1$ = 7.6 Hz, $J_2$ = 2.5 Hz, 2H, $CH_2$), 2.77−2.87 (m, 3H, $CH_2$ and CHH), 3.16 (dd, $J_1$ = 14.7 Hz, $J_2$ = 5.4 Hz, 1H, CHH), 3.41 (dd, $J_1$ = 8.2 Hz, $J_2$ = 5.4 Hz, 1H, CH), 7.40 (s, 1H, Ar), 7.45 (s, 1H, Ar). $^{13}$C NMR (75 MHz, $D_2O$, as a hydrobromide salt): $\delta$ 26.0, 32.3, 34.1, 53.2, 129.7, 131.2, 131.7, 132.8, 139.7, 170.6, 176.6.

**(*RS*)-2-Amino-3-(6-(2-carboxyethyl)-2,3-dichlorophenyl)propionic Acid (3g).** Yield 115 mg, 75%. Anal. Calcd for $C_{12}H_{13}NO_4Cl_2$: C, 47.08, H, 4.28, N, 4.58; Found: C, 46.65; H, 4.44; N, 4.46. $^1$H NMR (300 MHz, DMSO-$d_6$): $\delta$ 2.45 (t, $J$ = 7.7 Hz, 2H, $CH_2$), 2.85 (t, $J$ = 7.7 Hz, 2H, $CH_2$), 3.02 (dd, $J_1$ = 13.8 Hz, $J_2$ = 6.9 Hz, 1H, CHH), 3.27 (dd, $J_1$ = 13.8 Hz, $J_2$ = 8.3 Hz, 1H, CHH), 3.44 (t, $J$ = 7.6 Hz, 1H, CH), 7.13 (d, $J$ = 8.5 Hz, 1H, Ar), 7.38 (d, $J$ = 8.5 Hz, 1H, Ar).

**(*RS*)-2-Amino-3-(2-(2-carboxyethyl)-5-chlorophenyl)propionic Acid (3d).** A mixture of **11d** (395 mg, 1 mmol) and 48% HBr in water (6 mL) was refluxed for 2 h and evaporated under reduced pressure. Purification by preparative reversed-phase HPLC followed by recrystallization from water afforded the target amino acid as a white solid. Yield 173 mg, 64%. Anal. Calcd for $C_{12}H_{14}ClNO_4 \cdot 0.1H_2O$: C, 52.70; H, 5.23; N, 5.12. Found: C, 52.68; H, 5.20; N, 5.36. $^1$H NMR (300 MHz, $D_2O$): $\delta$ 2.64 (t, $J$ = 7.5 Hz, 2H, $CH_2$), 2.92 (t, $J$ = 7.5 Hz, 2H, $CH_2$), 3.04 (dd, $J_1$ = 14.7 Hz, $J_2$ = 8.7 Hz, 1H, CHH), 3.31 (dd, $J_1$ = 14.7 Hz, $J_2$ = 6.8 Hz, 1H, CHH), 3.89 (dd, $J_1$ = 8.7 Hz, $J_2$ = 6.8 Hz, 1H, CH), 7.22−7.29 (m, 3H, Ar). $^{13}$C NMR (75 MHz, $D_2O$): $\delta$ 26.4, 33.1, 34.8, 53.8, 128.4, 130.2, 131.1, 132.1, 134.5, 138.2, 171.3, 177.5.

**(*RS*)-2-Amino-3-(2-(2-carboxyethyl)-5-(hydroxymethyl)phenyl)propionic Acid (3e).** A mixture of **12** (163 mg, 0.36 mmol) in 48% aqueous HBr (2 mL) was refluxed for 1 h, and the solvent was removed in vacuo. Then water (2 mL) was added and the mixture was refluxed for additional 2 h and evaporated. Purification by reversed-phase HPLC afforded the target amino acid as a white solid. Yield 36 mg, 37%. Anal. Calcd for $C_{13}H_{17}NO_5$: C, 58.47; H, 6.97; N, 5.57. Found: C, 58.97; H, 7.04; N, 5.29. $^1$H NMR (300 MHz, $D_2O$): $\delta$ 2.45 (t, $J$ = 7.5 Hz, 2H, $CH_2$), 2.74 (t, $J$ = 7.3 Hz, 2H, $CH_2$), 2.85 (dd, $J_1$ = 15 Hz, $J_2$ = 8.8 Hz, 1H, CHH), 3.14 (dd, $J_1$ = 14 Hz, $J_2$ = 6.4 Hz, 1H, CHH), 3.70 (dd, $J_1$ = 8.8 Hz, $J_2$ = 6.0 Hz, 1H, CH), 4,34 (s, 2H, $CH_2$), 6,99 (s, 1H, Ar), 7.03 (d, $J$ = 8,7 Hz, 1H, Ar), 7.59 (d, $J$ = 8.3 Hz, 1H, Ar).

**Synthesis of the Compounds 3h−j.** Compounds **13−15** (0.5 mmol) were refluxed in 48% aqueous HBr and purified by the method described for compound **3d** to give the target amino acids **3h−j** as white solids.

**(*RS*)-2-Amino-3-(2-(2-carboxyethyl)-5-chloro-4-nitrophenyl)propionic Acid (3h).** Yield 92 mg, 58%. Anal. Calcd for $C_{12}H_{13}ClN_2O_6 \cdot 0.8H_2O$: C, 43.53; H, 4.44; N, 8.46. Found: C, 43.46; H, 4.28; N, 8.33. $^1$H NMR (300 MHz, DMSO-$d_6$): $\delta$ 2.56 (t, $J$ = 7.7 Hz, 2H, $CH_2$), 2.80−3.05 (m, 3H, $CH_2$ and CHH), 3.27 (dd, $J_1$ = 14.3 Hz, $J_2$ = 5.2 Hz, 1H, CHH), 3.52 (t, $J$ = 7.4 Hz, 1H, CH), 7.60 (s, 1H, Ar), 7.88 (s, 1H, Ar). $^{13}$C NMR (75 MHz, DMSO-$d_6$): $\delta$ 26.1, 32.1, 33.9, 52.1, 122.1, 125.7, 132.7, 140.4, 140.9, 146.2.

**(*S*)-2-Amino-3-(2-(2-carboxyethyl)-5-chloro-4-nitrophenyl)propionic Acid [(*S*)-3h] and (*R*)-2-Amino-3-(2-(2-carboxyethyl)-5-chloro-4-nitrophenyl)propionic Acid [(*R*)-3h].** The chiral separation of (*RS*)-**3h** was performed using a ligand-exchange Sumichiral OA500 HPLC column,[18,19] as described in HPLC Procedures. Appropriate fractions were pooled and evaporated. In order to remove

the buffer salts, the residues were dissolved in 1 M HCl and purified by reverse-phase FC eluted with methanol/15 mM AcOH. Recrystallizations from water gave isomers with sufficient purity. The $^1$H NMR data of *S*- and *R*-enantiomers of **3h** were identical with the data for (*RS*)-**3h** reported above. (*S*)-**3h**. Yield 17%, 97% ee; $\Delta\varepsilon$ (205 nm) = 0.46 m$^2$/mol. Anal. Calcd for $C_{12}H_{13}ClN_2O_6 \cdot 1H_2O$: C, 43.06; H, 4.52; N, 8.37. Found: C, 43.23; H, 4.20; N, 8.15. (*R*)-**3h**. Yield 21%, 95% ee; $\Delta\varepsilon$ (205 nm) = −0.44 m$^2$/mol. Anal. Calcd for $C_{12}H_{13}ClN_2O_6 \cdot 1H_2O$: C, 43.06; H, 4.52; N, 8.37. Found: C, 43.28; H, 4.22; N, 8.30.

**(*RS*)-2-Amino-3-(4-amino-2-(2-carboxyethyl)-5-chlorophenyl)propionic Acid (3i).** Yield 64 mg, 45%. Anal. Calcd for $C_{12}H_{15}N_2O_4Cl \cdot 0.35H_2O$: C, 49.19; H, 5.40; N, 9.56. Found: C, 49.03; H, 5.19; N, 9.43. $^1$H NMR (300 MHz, $D_2O$): $\delta$ 2.65 (t, $J$ = 7.2 Hz, 2H, $CH_2$), 2.88 (t, $J$ = 7.2 Hz, 2H, $CH_2$), 2.97 (dd, $J_1$ = 14.8 Hz, $J_2$ = 9.1 Hz, 1H, CHH), 3.26 (dd, $J_1$ = 14.8 Hz, $J_2$ = 5.8 Hz, 1H, CHH), 3.86 (t, $J$ = 8.8 Hz, 1H, CH), 6.86 (s, 1H, Ar), 7.19 (s, 1H, Ar); $^{13}$C NMR (75 MHz, DMSO-$d_6$): $\delta$ 26.9, 32.9, 35.5, 55.1, 115.1, 115.8, 123.8, 130.3, 139.1, 143.0, 166.9, 173.7.

**(*RS*)-4-(2-amino-2-carboxyethyl)-5-(2-carboxyethyl)-2-chlorobenzoic Acid (3j).** Yield 55 mg, 35%. Anal. Calcd for $C_{13}H_{14}NO_6Cl \cdot 1.4H_2O$: C, 45.80; H, 4.97; N, 4.11. Found: C, 45.46; H, 4.62; N, 4.03. $^1$H NMR (300 MHz, $D_2O$): $\delta$ 2.73 (t, $J$ = 7.4 Hz, 2H, $CH_2$), 2.99 (t, $J$ = 7.4 Hz, 2H, $CH_2$), 3.13 (dd, $J_1$ = 14.5 Hz, $J_2$ = 8.5 Hz, 1H, CHH), 3.41 (dd, $J_1$ = 14.5 Hz, $J_2$ = 5.8 Hz, 1H, CHH), 4.03 (t, $J$ = 8.5 Hz, 1H, CH), 7.38 (s, 1H, Ar), 7.55 (s, 1H, Ar). $^{13}$C NMR (75 MHz, DMSO-$d_6$): $\delta$ 26.4, 33.4, 34.9, 54.3, 128.9, 130.5, 130.9, 131.6, 138.6, 140.0, 166.9, 169.6, 173.4.

## ■ ASSOCIATED CONTENT

**Supporting Information.** Synthesis procedures and NMR data for all compounds except compounds investigated pharmacologically, experimental procedures for in vitro pharmacology, and results from X-ray crystallography. This material is available free of charge via the Internet at http://pubs.acs.org.

### Accession Codes

[†]PDB code for GluA2 ligand-binding domain (S1S2J) in complex with the antagonist (*S*)-2-amino-3-(2-(2-carboxyethyl)-5-chloro-4-nitrophenyl)propionic acid [(*S*)-3h] is 3TZA.

## ■ AUTHOR INFORMATION


### Corresponding Author

*Phone: (+45) 35 33 64 12. Fax: (+45) 35 33 60 01. E-mail: tnj@farma.ku.dk.

### Present Addresses

[‖]Department of Technology and Biotechnology of Drugs, Jagiellonian University Medical College, 9 Medyczna Street, 30-688 Krakow, Poland.

### Author Contributions

[#]E.S. and K.F. contributed equally to this work and are joint first authors.


## ■ ACKNOWLEDGMENT

The work was supported by the Danish Medical Research Council, the Alfred Benzon Foundation, GluTarget, Dansync, and Polish State Committee for Scientific Research. ESRF, Grenoble, France, is thanked for providing beamtime.

## ■ ABBREVIATIONS USED

AMPA, (*RS*)-2-amino-3-(3-hydroxy-5-methylisoxazol-4-yl)propionic acid; (*S*)-ATPO, (*S*)-2-amino-3-[5-*tert*-butyl-3-(phosphonomethoxy)isoxazol-4-yl]propionic acid; (*S*)-Br-HIBO, (*S*)-2-amino-3-(4-bromo-3-hydroxyisoxazol-5-yl)propionic acid; CNS, central nervous system; CNQX, 6-cyano-7-nitroquinoxaline-2,3-dione; CTZ, cyclothiazide; Glu, glutamate; GluA2-S1S2J, ligand binding domain of the GluA2 receptor subunit; iGluR, ionotropic glutamate receptor; KA, kainic acid; LBD, ligand binding domain; NMDA, *N*-methyl-D-aspartic acid; NS1209, 8-methyl-5-(4-(*N*,*N*-dimethylsulfamoyl)phenyl)-6,7,8,9,-tetrahydro-1*H*-pyrrolo[3,2-*h*]isoquinoline-2,3-dione-3-*O*-(4-hydroxybutyrate-2-yl)oxime; TEVC, two-electrode voltage clamp; $V_h$, TEVC holding potential

## ■ REFERENCES


(1) Traynelis, S. F.; Wollmuth, L. P.; McBain, C. J.; Menniti, F. S.; Vance, K. M.; Ogden, K. K.; Hansen, K. B.; Yuan, H.; Myers, S. J.; Dingledine, R. Glutamate receptor ion channels: structure, regulation, and function. *Pharmacol. Rev.* **2010**, *62*, 405–496.

(2) Bleakman, D.; Alt, A.; Nisenbaum, E. S. Glutamate receptors and pain. *Semin. Cell Dev. Biol.* **2006**, *17*, 592–604.

(3) Black, M. D. Therapeutic potential of positive AMPA modulators and their relationship to AMPA receptor subunits. A review of preclinical data. *Psychopharmacology* **2005**, *179*, 154–163.

(4) Kew, J. N.; Kemp, J. A. Ionotropic and metabotropic glutamate receptor structure and pharmacology. *Psychopharmacology* **2005**, *179*, 4–29.

(5) Rao, V. R.; Finkbeiner, S. NMDA and AMPA receptors: old channels, new tricks. *Trends Neurosci.* **2007**, *30*, 284–291.

(6) Hume, R. I.; Dingledine, R.; Heinemann, S. F. Identification of a site in glutamate receptor subunits that controls calcium permeability. *Science* **1991**, *253*, 1028–1031.

(7) Lomeli, H.; Mosbacher, J.; Melcher, T.; Hoger, T.; Geiger, J. R.; Kuner, T.; Monyer, H.; Higuchi, M.; Bach, A.; Seeburg, P. H. Control of kinetic properties of AMPA receptor channels by nuclear RNA editing. *Science* **1994**, *266*, 1709–1713.

(8) Fleming, J. J.; England, P. M. Developing a complete pharmacology for AMPA receptors: a perspective on subtype-selective ligands. *Bioorg. Med. Chem.* **2010**, *18*, 1381–1387.

(9) Jane, D. E.; Hoo, K.; Kamboj, R.; Deverill, M.; Bleakman, D.; Mandelzys, A. Synthesis of willardiine and 6-azawillardiine analogs: pharmacological characterization on cloned homomeric human AMPA and kainate receptor subtypes. *J. Med. Chem.* **1997**, *40*, 3645–3650.

(10) Greenwood, J. R.; Mewett, K. N.; Allan, R. D.; Martin, B. O.; Pickering, D. S. 3-Hydroxypyridazine 1-oxides as carboxylate bioisosteres: a new series of subtype-selective AMPA receptor agonists. *Neuropharmacology* **2006**, *51*, 52–59.

(11) Coquelle, T.; Christensen, J. K.; Banke, T. G.; Madsen, U.; Schousboe, A.; Pickering, D. S. Agonist discrimination between AMPA receptor subtypes. *NeuroReport* **2000**, *11*, 2643–2648.

(12) Banke, T. G.; Greenwood, J. R.; Christensen, J. K.; Liljefors, T.; Traynelis, S. F.; Schousboe, A.; Pickering, D. S. Identification of amino acid residues in GluR1 responsible for ligand binding and desensitization. *J. Neurosci.* **2001**, *21*, 3052–3062.

(13) Hogner, A.; Kastrup, J. S.; Jin, R.; Liljefors, T.; Mayer, M. L.; Egebjerg, J.; Larsen, I. K.; Gouaux, E. Structural basis for AMPA receptor activation and ligand selectivity: crystal structures of five agonist complexes with the GluR2 ligand-binding core. *J. Mol. Biol.* **2002**, *322*, 93–109.

(14) Bjerrum, E. J.; Kristensen, A. S.; Pickering, D. S.; Greenwood, J. R.; Nielsen, B.; Liljefors, T.; Schousboe, A.; Brauner-Osborne, H.; Madsen, U. Design, synthesis, and pharmacology of a highly subtype-selective GluR1/2 agonist, (*RS*)-2-amino-3-(4-chloro-3-hydroxy-5-isoxazolyl)propionic acid (Cl-HIBO). *J. Med. Chem.* **2003**, *46*, 2246–2249.

(15) Hogner, A.; Greenwood, J. R.; Liljefors, T.; Lunn, M. L.; Egebjerg, J.; Larsen, I. K.; Gouaux, E.; Kastrup, J. S. Competitive antagonism of AMPA receptors by ligands of different classes: crystal structure of ATPO bound to the GluR2 ligand-binding core, in comparison with DNQX. *J. Med. Chem.* **2003**, *46*, 214–221.

(16) Hamilton, G. S. Omega-[2-(alkyl)phenyl]-2-aminoalkanoic Acids as Antagonists of Excitatory Amino Acids Receptors. US 5,364, 876, 1994.

(17) Hamilton, G. S.; Huang, Z.; Patch, R. J.; Guzewska, M. E.; Elliott, R. L.; Borosky, S. A.; Bednar, D. L.; Ferkany, J. W.; Karbon, E. W. Phosphonoethylphenylalanine derivatives as novel antagonists of non-NMDA ionotropic glutamate receptors. *Bioorg. Med. Chem. Lett.* **1992**, *2*, 1269–1274.

(18) Oi, N.; Kitahara, H.; Kira, R. Direct separation of enatiomers by high-performance liquid chromatography on a new chiral ligand-exchange phase. *J. Chromatogr., A* **1992**, *592*, 291–296.

(19) Miyazawa, T.; Minowa, H.; Imagawa, K.; Yamada, T. Enantiomeric separation of non-protein amino acids by chiral ligand-exchange high-performance liquid chromatography. *Anal. Lett.* **1997**, *30*, 867–882.

(20) Armstrong, D. W.; Liu, Y.; Ekborg-Ott, K. H. A covalently bonded teicoplanin chiral stationary phase for HPLC enantioseparations. *Chirality* **1995**, *7*, 474–497.

(21) Berthod, A.; Liu, Y.; Bagwill, C.; Armstrong, D. W. Facile liquid chromatographic enantioresolution of native amino acids and peptides using a teicoplanin chiral stationary phase. *J. Chromatogr., A* **1996**, *731*, 123–137.

(22) Møller, E. H.; Egebjerg, J.; Brehm, L.; Stensbøl, T. B.; Johansen, T. N.; Madsen, U.; Krogsgaard-Larsen, P. Resolution, absolute stereochemistry, and enantiopharmacology of the GluR1−4 and GluR5 antagonist 2-amino-3-[5-*tert*-butyl-3-(phosphonomethoxy)-4-isoxazolyl] propionic acid. *Chirality* **1999**, *11*, 752–759.

(23) Madsen, U.; Brauner-Osborne, H.; Frydenvang, K.; Hvene, L.; Johansen, T. N.; Nielsen, B.; Sanchez, C.; Stensbøl, T. B.; Bischoff, F.; Krogsgaard-Larsen, P. Synthesis and pharmacology of 3-isoxazolol amino acids as selective antagonists at group I metabotropic glutamic acid receptors. *J. Med. Chem.* **2001**, *44*, 1051–1059.

(24) Legrand, M.; Rougier, M. J. Application of the Optical Activity to Stereochemical Determinations. In *Determination of Configurations by Dipole Moment, CD or ORD*; Kaagan, H. B., Ed.; Stereochemistry: Fundamentals and Methods, Vol. 2; Georg Thieme Publishers: Stuttgart, Germany, 1977; pp 33−183.

(25) Frandsen, A.; Pickering, D. S.; Vestergaard, B.; Kasper, C.; Nielsen, B. B.; Greenwood, J. R.; Campiani, G.; Fattorusso, C.; Gajhede, M.; Schousboe, A.; Kastrup, J. S. Tyr702 is an important determinant of agonist binding and domain closure of the ligand-binding core of GluR2. *Mol. Pharmacol.* **2005**, *67*, 703–713.

(26) Ahmed, A. H.; Thompson, M. D.; Fenwick, M. K.; Romero, B.; Loh, A. P.; Jane, D. E.; Sondermann, H.; Oswald, R. E. Mechanisms of antagonism of the GluR2 AMPA receptor: structure and dynamics of the complex of two willardiine antagonists with the glutamate binding domain. *Biochemistry* **2009**, *48*, 3894–3903.

(27) Madsen, U.; Bang-Andersen, B.; Brehm, L.; Christensen, I. T.; Ebert, B.; Kristoffersen, I. T.; Lang, Y.; Krogsgaard-Larsen, P. Synthesis and pharmacology of highly selective carboxy and phosphono isoxazole amino acid AMPA receptor antagonists. *J. Med. Chem.* **1996**, *39*, 1682–1691.

(28) Pøhlsgaard, J.; Frydenvang, K.; Madsen, U.; Kastrup, J. S. Lessons from more than 80 structures of the GluA2 ligand-binding domain in complex with agonists, antagonists and allosteric modulators. *Neuropharmacology* **2011**, *60*, 135–150.

(29) Armstrong, N.; Gouaux, E. Mechanisms for activation and antagonism of an AMPA-sensitive glutamate receptor: crystal structures of the GluR2 ligand binding core. *Neuron* **2000**, *28*, 165–181.

(30) Menuz, K.; Stroud, R. M.; Nicoll, R. A.; Hays, F. A. TARP auxiliary subunits switch AMPA receptor antagonists into partial agonists. *Science* **2007**, *318*, 815–817.

(31) Cruz, L. A.; Estebanez-Perpina, E.; Pfaff, S.; Borngraeber, S.; Bao, N.; Blethrow, J.; Fletterick, R. J.; England, P. M. 6-Azido-7-nitro-1,4-dihydroquinoxaline-2,3-dione (ANQX) forms an irreversible bond to the active site of the GluR2 AMPA receptor. *J. Med. Chem.* **2008**, *51*, 5856–5860.

(32) Kasper, C.; Pickering, D. S.; Mirza, O.; Olsen, L.; Kristensen, A. S.; Greenwood, J. R.; Liljefors, T.; Schousboe, A.; Watjen, F.; Gajhede, M.; Sigurskjold, B. W.; Kastrup, J. S. The structure of a mixed GluR2 ligand-binding core dimer in complex with (*S*)-glutamate and the antagonist (*S*)-NS1209. *J. Mol. Biol.* **2006**, *357*, 1184–1201.

(33) Robert, A.; Armstrong, N.; Gouaux, J. E.; Howe, J. R. AMPA receptor binding cleft mutations that alter affinity, efficacy, and recovery from desensitization. *J. Neurosci.* **2005**, *25*, 3752–3762.